Population histories of the United States revealed through fine-scale migration and haplotype analysis

Chengzhen L. Dai[1], Mohammad M. Vazifeh[2], Chen-Hsiang Yeang[3], Remi Tachet[2], Miguel G. Vilar[4], Mark J. Daly[5,6,7,8], Carlo Ratti[2]*, Alicia R. Martin[6,7,8]*†

[1] Department of Electrical Engineering and Computer Science, Massachusetts Institute of Technology, Cambridge, MA 02139, USA

[2] Senseable City Lab, Massachusetts Institute of Technology, Cambridge, MA 02139, USA

[3] Institute of Statistical Science, Academia Sinica, Nankang, Taipei, Taiwan

[4] Genographic Project, National Geographic Society, Washington, DC 20036, USA

[5] Institute for Molecular Medicine Finland (FIMM), University of Helsinki, Helsinki, Finland

[6] Analytic and Translational Genetics Unit, Massachusetts General Hospital, Boston, MA 02114, USA

[7] Program in Medical and Population Genetics, Broad Institute of Harvard and MIT, Cambridge, MA 02142, USA

[8] Stanley Center for Psychiatric Research, Broad Institute of Harvard and MIT, Cambridge, MA 02142, USA

*These authors jointly supervised this work

†Corresponding author: armartin@broadinstitute.org

Abstract

The population of the United States is shaped by centuries of migration, isolation, growth, and admixture between populations of global origins. Here, we assemble a comprehensive view of recent population history by studying the ancestry and population structure of over 32,000 individuals in the US using genetic, ancestral birth origin, and geographic data. We identify migration routes and barriers that reflect historical demographic events. We also uncover the spatial patterns of relatedness in subpopulations through the combination of haplotype clustering, ancestral birth origin analysis, and local ancestry inference. These patterns include substantial structure and heterogeneity in Hispanics/Latinos, isolation-by-distance in African Americans, elevated levels of relatedness and homozygosity in Asian immigrants, and fine-scale structure in European descents. Furthermore, quantification of familial birthplaces recapitulates historical immigration waves at high resolution. Taken together, our results provide detailed insights into the genetic structure and demographic history of the diverse US population.

Significance Statement

The population of the United States has globally diverse ancestors and a complex history. Despite previous studies of genetic diversity in the US, population history for many groups still remains ambiguous. Here, we study the DNA of over 32,000 US individuals who participated in the National Geographic Genographic Project. By combining analyses of migration, haplotype sharing, and ancestral birthplaces, we reconstruct demographic histories at fine-scale resolution. Among European Americans, Hispanics/Latinos, and African Americans, we disentangle patterns of immigration, within-country migration, and admixture. We also characterize the typically overlooked population history of Asian Americans. Overall, this study sheds light on the complex population histories detailed in the DNA of people living in the US.

Keywords: population genetics, human history, human genomics, USA

Introduction

The United States population is a diverse collection of global ancestries shaped by migration from distant continents and admixture of migrants and Native Americans. Throughout the past few centuries, continuous migration and gene flow have played major roles in shaping the diversity of the US. Mixing between groups that have historically been genetically and spatially distinct have resulted in individuals with complex ancestries while within-country migration have led to genetic differentiation.[1–7]

Previous genetics studies of the US population have sought to disentangle the relationship between the genetic ancestry and population history of African Americans, European Americans, and Hispanics/Latinos. In African Americans, proportions of African, European, and Native American ancestry vary across the country and reflect migration routes, slavery, and patterns of segregation between states.[2,3,8] European American ancestry is characterized by both mixing between different European populations as well as admixture with non-European population.[6,9,10] Isolation and expansions in certain European population have also resulted in founder effects.[11–13] The mixing of European settlers with Native Americans have contributed to large variations in the admixture proportions of different Hispanic/Latino populations.[1,4,5] Among Hispanics/Latinos, Mexicans and Central Americans carry more Native American ancestry; Puerto Ricans and Dominicans have higher African ancestry; and Cubans have strong European ancestry.[1,4] Although much effort has been made to understand the genetic diversity in the US, fine-scale patterns of demography, migration, isolation, and founder effects are still being uncovered with the growing scale of genetic data, particularly for Latin American and African descendants with complex admixture history.[14,15] At the same time, there has been little research on the population structure of individuals with East Asian, South Asian, and Middle Eastern ancestry in the US.

In addition to being of anthropological interest, understanding fine-scale human history and its role in shaping genetic variation is also important for interpreting the genetic basis of biomedical traits. Currently, these roles are best understood in European populations due to Eurocentric biases in studies.[16,17] Consequently, translational interpretability gaps are evident in non-European populations: more variants of unknown significance are identified via genetic testing;[18] polygenic risk scores for complex disease risks are much less accurate;[17,19] and false positive genetic misdiagnoses are more common.[20] Thus, studies of diverse, heterogeneous populations

offer substantial value to both our understanding of population history and biomedical outcomes.[21]

In this study, we comprehensively explore the population structure and migration history of over 32,000 genotyped individuals in the US who partook in the second phase of the National Geographic Genographic Project. The Genographic Project began in 2005 as a not-for-profit public participation research initiative to study human migration history, originally using Y chromosome and mitochondrial markers.[22] More recently, it expanded to include autosomal variants.[23] Here, we identify patterns of genetic ancestry and haplotype sharing among the project participants. We combine these patterns with ancestral birth origin records and geographic information to uncover recent demographic and migration trends. Taken together, we provide insights into the ancestral origins and complex population histories in the US.

Results

Genetic ancestry and diversity across the United States

To assess proportions and diversity of continental ancestries among individuals in the Genographic Project, we merged genotype data with the 1000 Genomes Project data (Auton et al, 2015) as reference populations, and performed PCA and ADMIXTURE (at K = 2 through K = 9) on the Genographic individuals.[24,25] Since self-reported ethnicity does not necessarily reflect genetic ancestry, we sought to objectively assign continental-level ancestry to Genographic individuals. We first trained a Random Forest classification algorithm on the first 10 principal components (PCs) of the 1000 Genome Project individuals using super population classifications (EUR = European, AMR = Admixed American, AFR = African, EAS = East Asian, SAS = South Asian) as ancestry labels (**Figure 1A-B; Figure S1**). We then used this trained model to assigned continent-level ancestry to each individual in the Genographic cohort at 90% confidence (**Table S1**; **Methods and Materials**).

Regional differences in genetic ancestry proportions correspond to historical demographic trends. We evaluated the admixture proportions of classified individuals across the four designated US Census regions: South, Northeast, Midwest, and West (**Figure 1C; Figure S2**). Individuals of European descent make up the majority (78.5%) of the Genographic cohort and are the most prevalent in the Midwest (82.8% of individuals in the Midwest; $P<0.01$, Fisher's

exact test; **Table S1**). Individuals classified as having African ancestry are most common in the South (3.2%), followed by the Northeast (3.0%). individuals of Native American ancestry are most prominent in the West and South (9.7% and 7.8% of total individuals in the West and South, respectively; $P<0.05$, Fisher's exact test). East Asians mostly reside in the West (2.1%), while South Asians are most abundant in the Northeast (1.0%). A total of 3,028 individuals (9.3% of total) did not meet the classification threshold, although many have ancestry patterns similar to other European individuals (**Figure 1C; Table S1**). The inability to classify these individuals may be due to the complex and variable admixture profiles of certain populations such as Hispanics/Latinos.

To uncover population substructure, we performed dimensionality reduction with Uniform Manifold Approximation and Projection (UMAP) on the first 20 PCs of a combined Genographic and 1000 Genomes Project dataset.[26,27] By leveraging multiple PCs at once, UMAP can disentangle subcontinental structure (**Figure 1D-E; Figure S3-S4**). Similar to previous analysis,[27] populations in the 1000 Genomes Project form distinct clusters corresponding to ancestry and geography. The Genographic individuals project into several clusters, overlapping with the 1000 Genomes Project clusters (**Figure 1D-E**). Consistent with the PCA and ADMIXTURE analysis, the largest clusters correspond to European ancestry and cluster closely with the 1000 Genomes CEU and GBR populations (CEU=Utah Residents with Northern and Western European Ancestry, GBR=British in England and Scotland).

While UMAP is a visualization tool with no direct interpretation on genetic distance, the continuum of points connecting UMAP clusters reflects the varying degrees of estimated admixture between different continental ancestries. In particular, the complex population structure of Hispanics/Latinos is shown by the points spanning between the clusters of European, Native American, and African ancestry. Coloring of these points based on ancestry proportions affirms the relationship between the degree of admixture and their relative position between reference clusters. Interestingly, African American individuals from both datasets form a single continuum from the European cluster to the Yoruba (YRI) and Esan (ESN) populations of Nigeria in the 1000 Genomes Project, indicative of the West African origins of most African Americans. This observation is consistent with and further expands the previous finding that the African tracts in the admixed 1000 Genomes populations of ACB and ASW were previously found to be similar to the Nigerian YRI and ESN populations.[2,19]

Population differentiation and migration rate inference across the United States

To better understand the relationship between genetics and geography, we investigated migration rates for genetically inferred Europeans, African Americans, and Hispanic/Latinos across the United States. We excluded East Asians and South Asians due to small sample size and limited our analysis to the contiguous 48 states. We inferred effective migration rates with the estimating effective migration surfaces (EEMS) method,[28] which statistically characterizes genetic differentiation via resistance distance across non-homogenous landscapes. By overlaying a dense regular grid of demes and measuring genetic dissimilarities between neighboring demes, EEMS quantifies and visualizes areas with high relative rates of effective migration (colored in blue) and areas with low relative rates of effective migration (also called migration barriers and colored in dark orange).

The inferred migration rates for African Americans reveal genetic signatures of historical demographic events (**Figure 2A; Figure S5**). Along the Atlantic coast from the Florida Panhandle to southern Maine, we find high effective migration rates, indicating the constant migration and similar effective population sizes of African Americans in these states. However, we also observe a strong north-south barrier to migration starting along the Appalachian Mountain Range, continuing north up the Mississippi River, and extending west across the rest of the country. This migration barrier, along with the migration barrier spanning Texas and New Mexico, reveals a pattern of isolation-by-distance that is consistent with the Great Migration from from the 1910s to the 1960s in which an estimated 6 million African Americans migrated out of the South to cities across the Northeast, Midwest and West.[8,29]

A highly complex pattern of migration exists amongst Hispanics/Latinos with varying migration rates across the country, capturing regional patterns of genetic similarity. Hispanics/Latinos in the southwestern states including two regions bordering Mexico—one in California and another extending from New Mexico to Texas—exhibit high effective migration rates and are separated by a migration barrier in Arizona (**Figure 2B; Figure S5**). These two distinct regions likely reflect known differences in northward migration from east versus west Mexico.[9,30] Along the Atlantic coast from Florida to New York, effective migration has also been fluid. However, barriers to migration are observed west of the Atlantic coast to the Mississippi River, likely resulting from varying admixture proportions.

186 The pattern of migration for Europeans captures subcontinental structure. Elevated migration
187 rates are observed across most of the country, except for many states in the Midwest and along
188 the Atlantic coast. We find low effective migration rates surrounding Minnesota and North
189 Dakota, potentially due to the genetic dissimilarity of Finnish and Scandinavian ancestry
190 abundant in the region (**Figure 2C; Figure S5**).[9] We also find reduced migration rates across
191 Ohio, West Virginia, and Virginia, suggesting the existence of genetic differentiation along the
192 Appalachian Mountains. Many of the major cities, such as Chicago, Philadelphia, and Miami,
193 are also barriers to migration, perhaps due to higher admixture proportions within cities. The
194 migration barrier encompassing metropolitan New York City may be explained in part by the
195 presence of divergent European populations, such as Ashkenazi Jews (**Figure 2C**).
196
197 **Coupling fine-scale haplotype clusters and multigenerational birth records uncovers**
198 **distinct subcontinental structure**
199 To disentangle more recent and subtle population structure, we performed identity-by-descent
200 (IBD) clustering on the Genographic cohort and annotated clusters using multigenerational self-
201 reported birth origin data. We first built an IBD network from pairwise IBD sharing among 31,783
202 unrelated individuals. In this network, vertices represent individuals and edges represent the
203 cumulative IBD (in centimorgans, cM) between pairs of individuals. We employed the Louvain
204 method, a greedy heuristic algorithm, to recursively partition vertices in the graph into clusters
205 that maximize modularity at each level of hierarchy.[9,31] The clusters of individuals resulting from
206 each iteration can be interpreted as having greater amounts of cumulative IBD shared between
207 individuals within the cluster than with individuals outside of the cluster. At the first level of
208 hierarchy, the full IBD network separated into three clusters: non-European ancestry, Southern
209 Europeans and Ashkenazi Jews, and the rest of the Europeans. Further partitioning, up to four
210 levels of hierarchy, produced clusters with more subcontinental structure. 98% of the 3,028
211 individuals that were not classified by our Random Forest model were assigned to a haplotype
212 cluster, affirming the power of haplotype clustering for detecting fine-scale structure. No single
213 cluster was overrepresented by unclassified individuals, as unclassified individuals comprised of
214 8-11% of each cluster.
215
216 To aid in the interpretation of the clusters, we merged clusters with low genetic differentiation
217 ($F_{ST} < 0.0001$) at the lowest level of hierarchy, resulting in a final set of 25 clusters (**Table 1**).
218 We annotated each cluster based on ancestral birth origin and ethnicity data and constructed a
219 neighbor-joining tree based on the F_{ST} values (**Figure 3**). As expected, F_{ST} values are smallest

220 between European subpopulations (F_{ST}=0.0001-0.003) and greatest between clusters of
221 different continental ancestries (F_{ST}=0.002-0.09).
222
223 Genetic and geographic diversity is greatest amongst Hispanic/Latino haplotype clusters. We
224 identified a total of five Hispanic-related clusters. The largest of these cluster (n=810) is strongly
225 associated with south Florida (OR = 10.4; p = 2.5e-25; **Figure 4**, **Table S4**) but is also found in
226 California, and Texas (OR ≥ 2; p < 0.05). No single ancestral birthplace characterizes this
227 cluster, as the US, Mexico, and Cuba each make up more than 10% of the birth origin labels.
228 Proportions of European ancestry tracts inferred with RFMix[32] are higher in this cluster (mean =
229 72.7%, sd=20.4%) than in the other Hispanic/Latino clusters (mean = 48.0% - 67.4%). Puerto
230 Ricans characterize a substantial proportion of another Hispanic/Latino cluster associated with
231 Florida (OR > 4), as well as New York City (OR > 5). Unlike the other Hispanic clusters, the
232 Puerto Rican cluster shares the same branch on the F_{ST} tree as the African American clusters,
233 likely due to high proportions of African ancestry (mean = 11.2%, sd = 9.0%) among Puerto
234 Ricans.
235
236 Three distinct clusters of Hispanics were found in the Southwest (**Figure 4**): one strongly
237 associated with New Mexico (OR > 4; p < 0.05), another primarily in Texas (OR > 3; p < 0.05),
238 and the third associated with Southern California (OR > 2; p < 0.05). Combined with the EEMS
239 analysis, these clusters confirm our observation of parallel migration routes from east and west
240 Mexico into Southwestern United States. While the genetic differentiation of these three clusters
241 are subtle (F_{ST}=0.001-0.003), ancestral birth origin patterns and local ancestry proportions for
242 these clusters reveal meaningful dissimilarities. Whereas the majority of Hispanics in New
243 Mexico report US ancestral birth origins through grandparents, the recent ancestors of
244 Hispanics in Texas are predominantly from Mexico. Nonetheless, these two clusters share
245 similar local ancestry proportions with only slight genetic dissimilarity that result in a moderate
246 decrease in migration rate (from darker blue to light blue in **Figure 2B**). The reduced migration
247 rate along the Texas-Mexico border may be caused by more recent immigrants. Unlike the
248 Hispanic clusters associated with New Mexico and Texas, the Hispanics in California cluster
249 contain greater proportions of ancestors from Central and South American (e.g., Colombia and
250 El Salvador). Proportions of Native American ancestry is also highest in this cluster (**Figure 4**).
251 Taken together, these two differences further explain the presence of the migration barrier in
252 Arizona between the Hispanics in the California and the Hispanics in New Mexico.
253

Historical immigration of Europeans into the US occurred in successive waves, with Northern and Western Europeans making up one wave from the 1840s to 1880s and another wave comprising of Southern and Eastern Europeans occurring from the 1880s to 1910s.[33] Consistent with this immigration pattern, haplotype clusters with ancestries from Northwest and Central Europe have higher proportions of US ancestral birth origins than haplotype clusters from Southern and Eastern Europe, suggesting earlier immigration (**Figure 5**). The two clusters with the highest proportion (>75%) of US ancestral birth origin ("Northwest Europe 1" and "Northwest Europe 2") have approximately 4.5% of UK ancestral origins. The Central European cluster and the Irish cluster both have approximately 66.1% to 68.5% of US grandparental origins, respectively. In contrast, the US makes up only 62.2% and 34.5% of grandparental birth origin for the clusters of Southern Europeans and Eastern Europeans, respectively.

Unlike the larger European clusters, the smaller European clusters reflect the structure of more recent immigrants and genetically isolated populations. The geographic distribution of these subpopulations are more concentrated, and their ancestral birth origin proportions are overrepresented by specific countries and ethnicities (**Figure 6**). For example, Finns and Scandinavians are abundant in the Upper Midwest and Washington; French Canadians are found in the Northeast; Acadians are present in the Northeast and Louisiana; and Italians, Greeks, Ashkenazi Jews, and Admixed Jews are mostly located in the metropolitan area of New York City. Of the European clusters, median cumulative IBD sharing and cROH lengths are highest amongst Ashkenazi Jews (31.8cM and 11.3 Mb, respectively; **Table 1**). The two Jewish-related clusters were identified using self-reported ancestral ethnicity data rather than birth origin data, since Jewish ancestry is not specific to any single location. Jewish ancestry, particularly Ashkenazi Jewish ancestry, was more consistently reported on both sides of the family in the larger Jewish cluster ("Ashkenazi Jewish"), suggesting that individuals are more admixed in the smaller cluster ("Admixed Jewish").

We inferred two haplotype clusters of African Americans separated along a north-south cline, recapitulating the EEMS migration barrier inference. One cluster is primarily distributed amongst the northern and western states ("African Americans North") while the other is distributed amongst the states southeast of the Appalachian Mountains ("African Americans South") **(Figure S7)**. The proportion of US birth origin is higher in the northern cluster than the southern cluster, further evidence of isolation by distance amongst African Americans in the north.[8] These two clusters share similar cROH lengths but differ in admixture proportions and median IBD

288 sharing, pointing to a cluster with consistent African American ancestors and a cluster with more
289 admixed ancestors. Median IBD sharing is higher amongst African Americans in the south
290 (median IBD = 19.6 cM, median cROH = 3.3 Mb) than in the north (median = 15.9 cM, **Table 2**)
291 while the average proportion of African ancestry is higher in the northern cluster than the
292 southern cluster.
293
294 Smaller haplotype clusters in the Genographic cohort reflect more recent immigration of South,
295 Southeast, and East Asian individuals to the US, which grew rapidly in the mid-20th Century
296 after the passage of laws eliminating national origin quotas.[34] We identified four clusters with
297 birth origins enriched from Asia (**Figure S8**). The recency of immigration among these clusters
298 is indicated by the less than 30% of ancestral birth origins coming from the US. Geographically,
299 individuals in these clusters primarily reside in major cities. East Asians predominantly inhabit
300 the metropolitan areas of coastal states in the West and Northeast (OR > 2), while South Asians
301 are strongly associated with the Northeast (OR > 2.5). Southeast Asians (OR > 2.5) are
302 enriched in the west but are also associated with the Carolinas and Ohio. Despite its small size,
303 the cluster of Middle Eastern individuals reflects many of the known demographic patterns of
304 Arab Americans, as individuals in this cluster are primarily of Lebanese origin and are
305 distributed in the Northeast as well as metropolitan Detroit. cROH lengths are particularly long
306 for South Asians (median cROH = 10.3 cM), Southeast Asians (median cROH = 7.8 cM), and
307 Middle Easterners (median cROH = 8.2 cM), potentially reflecting inbreeding patterns found in
308 their ancestral regions.[35]
309
310
311 **Discussion**
312
313 As the US population is becoming increasingly diverse, genomic studies are simultaneously
314 growing in scale and relevance; to increase scientific and ethical parity, these studies must
315 therefore move beyond the current practice of evaluating genetically homogenous groups in
316 isolation.[17] Here, we provide an integrative framework for analyzing population structure in
317 ancestrally heterogeneous individuals. Using data from the National Geographic Genographic
318 Project, we untangled the recent demographic histories of European, African American,
319 Hispanic/Latino, and Asian populations in the US by evaluating their admixture proportions,
320 migration rates, haplotype sharing, and ancestral birth origins.
321

322 Our comprehensive approach has allowed us to capture spatial patterns of gene flow within and
323 between subpopulations that are difficult to infer from a single method alone. For example,
324 EEMS is limited in identifying unique subpopulations, while haplotype clustering cannot assign
325 admixed individuals partial membership to multiple clusters. An integrative approach can thus
326 enable greater insights into populations with complex histories, such as recently admixed US
327 Hispanics/Latinos.
328
329 Consistent with prior studies,[4,10] the recent demographic history of Hispanic/Latino populations
330 is complex. Large variations in admixture proportions within and between subpopulations are
331 reflected by US Census Data and can likely be explained by numerous inferred migration
332 barriers. For example, regional differences in the Southwest are highlighted by an inferred
333 migration barrier in Arizona and distinct haplotype clusters surrounding this region. These
334 differences are likely due to higher proportions of Native American ancestry as well as more
335 Central and South American origins in the California Hispanic cluster compared to other
336 southwestern Hispanic/Latinos. Interestingly, although the New Mexico Hispanic/Latino cluster
337 is distinct from the Texan cluster, high levels of gene flow are inferred from southern New
338 Mexico to central Texas, suggesting that certain individuals in these two clusters are genetically
339 similar and may share an ancestral origin (i.e. Mexico). In contrast, those in northern New
340 Mexico are more genetically differentiated, as indicated by a migration barrier, but share the
341 same cluster; these are likely *Nuevomexicanos*, descendants of Spanish colonial settlers.
342
343 The fine-scale population structure of African Americans also reflects known historical events
344 following the transatlantic slave trade, during which millions of West Africans were forcibly
345 moved to the Americas. Subsequently, the movement of African Americans during the Great
346 Migration has been shown to correlate with current patterns of relatedness across US census
347 regions.[8] Our results show barriers to migration and gene flow at fine-scale, particularly along
348 the Appalachian Mountains. A north-south migration barrier is also present west of the
349 Mississippi River, and is further supported by the north-south locations of two African American
350 clusters that emphasize this divide. The southern African American cluster contains more recent
351 ancestors outside the US, particularly of Caribbean origin, than the northern African American
352 cluster. These genetic signatures illustrate the impact of recent migration patterns on modern
353 population structure.
354

Our ability to identify population structure for certain ancestries is subject to participation among individuals from those groups. In particular, individuals with Asian ancestries account for over 5% of US population, but they are underrepresented in US population genetics studies, hindering the investigation of their ancestry in prior studies.[9] Our analyses of East Asian, Southeast Asian, South Asian, and Middle Eastern populations therefore provide initial insights into their genetic structure. The ancestral origins and geographic distributions of these clusters are consistent with US Census reports. Since these populations descend from more recent immigrants, the observed patterns of homozygosity within several of these clusters likely reflect consanguinity patterns in some of their ancestral regions. Specifically, the long cROH in South Asians may reflect endogamy for example related to the caste system in India, while similar patterns among the Middle Eastern and Southeast Asian clusters may be capturing consanguineous marriage practices in those regions.[36–38] Given the small size of these clusters, however, further studies with larger data are needed.

Population history in the US is best characterized among the most populous European descent individuals. Genetic diversity tends to be highest in more densely populated regions, likely due to the presence of multiple subpopulations in the same place. Many of the European subpopulations we identified are similar to those previously found—e.g., French Canadians, Acadians, Scandinavians, Jews (Supplementary Discussion).[9] The geographic distribution of these subpopulations, particularly those that are more genetically diverged, overlap in the metropolitan areas in the Northeast, Midwest, and California.

The emergence of biobank-scale genomic data is enabling more complete pedigrees,[39] greater discoveries of fine-scale population structure, and more precise insights into health-related associations. An estimated 26 million people have taken a direct-to-consumer ancestry test,[40] indicating widespread interest in ancestry and heritable factors. As participation in genetic studies increase, especially in the US with the All of Us Research Program, so does the need for inferring increasingly granular demographic history in study cohorts. Understanding such genetic structure is important to account for stratification, prevent the overgeneralization of results, and avoid exacerbating existing biases.[16,17] This study demonstrates the potential of coupling genetic data with geographic and birth origin data to reconstruct such demographic histories, particularly in a large and heterogeneous population.

Materials and Methods

Human Subjects

The Genographic Project and Geno 2.0 Project received full approval from the Social and Behavioral Sciences Institutional Review Board (IRB) at the University of Pennsylvania Office of Regulatory Affairs on April 12, 2005. The IRB operates in compliance with applicable laws, regulations, and ethical standards necessary for research involving human participants. All data in this study came from participants that consented to have their results be used in scientific research. All data was deidentified.

In addition to genotype data, participants also provided information on geographic location, ancestral birth origin, and self-declared ethnicity. Geographic location was collected in the form of postal code. We limited our analysis to include only individuals who provided valid geographic location. Both ancestral birth origin data and self-declared ethnicity data were collected up to the grandparents of the participants. Approximately 60% of individuals provided complete pedigrees.

Genotyping and Quality Control

Participants of the Genographic project were sequenced with the GenoChip array,[23] a Illumina iSelect HD custom genotyping bead array with approximately 150,000 Ancestry Informative Markers from autosomal DNA, Y chromosome DNA, and mitochondrial DNA.

Raw genotype data was quality controlled (QC) using PLINK v1.90b3.39.[41] We filtered for samples with ≤ 0.1 missingness, sites with = 0.0 missingness, and MAF ≥ 0.05. After QC, 32,589 individuals and 108,003 sites remained.

Principal Component Analysis

We performed principal component analysis on the quality-controlled samples using FlashPCA version 2.0.[25] We included the genotypes of all 2,504 individuals from the 1000 Genomes Project as reference samples. We first found the subset of SNPs (108,003) that were shared between the Genographic samples and the 1000 Genomes Project samples. We next computed PCs across all 108,003 sites for all 1000 Genome Project individuals. Using the resulting PCs, we then projected the Genographic individuals on the same principal component space.

421 **Continental Ancestry Assignment**
422 We assigned continental ancestry to each individual in the Genographic dataset by leveraging
423 the PCs and known super population assignment (AFR=African, EUR=European, EAS=East
424 Asian, AMR=American, and SAS=South Asian) of each individual in the 1000 Genome Project.
425 We trained a random forest classifier on the first 10 PCs of the 1000 Genome Project samples
426 and assigned ancestry to all of the Genographic samples at 90% probability based on the
427 model. All unassigned ancestries were considered "other" (OTH).
428
429 **Genetic Ancestry Proportion Estimation**
430 We estimated admixture proportions using ADMIXTURE.[24] Similar to the PCA analysis, we
431 included the genotypes of all individuals from the 1000 Genomes Project and used the subset of
432 SNPs shared between the Genographic and 1000 Genomes Project datasets. We ran
433 ADMIXTURE for k=3-10 by first analyzing the 1000 Genomes Project in unsupervised mode to
434 learn allele frequencies and obtain ancestry proportions. Then, we projected the Genographic
435 samples onto the learned allele frequencies of the 1000 Genome Project samples to obtain the
436 learned clusters and ancestry proportions. We chose k = 5 as the most stable and best
437 representation of ancestry.
438
439 **UMAP**
440 We applied the Uniform Manifold Approximation and Projection (UMAP) method to visualize
441 subcontinental structure.[26,27] We first combined the PCs for the Genographic samples and the
442 1000 Genome Project samples, from the PCA analysis above, into one dataset. We then used
443 the UMAP implementation in Python to dimensionally reduce the first 20 PCs from the joint
444 dataset into a two-dimensional plot. We tested various parameter choices for UMAP and found
445 that the default nearest neighbor value of 15 and the minimum distance values of 0.5 delivered
446 the clearest result.
447
448 To help with interpretability, we colored the 1000 Genome Project samples in the UMAP
449 projection based on their country level assignments (Figure 1C left). We also visualized the
450 Genographic samples in the UMAP projection by coloring each sample based on their ancestry
451 proportions from ADMIXTURE (Figure 1C right). Specifically, the color (RGB value) of each
452 sample is a linear combination of the sample's ancestry proportions and the RGB values of
453 each ancestry's color (EUR = red, AFR = yellow, NAM = green, EAS = blue, SAS = purple).
454

455 **Genetic Relatedness**

456 We used KING v2.0 to identify the set of unrelated individuals within the Genographic dataset
457 separated by at least two degrees of relatedness.[42] In total, 806 individuals had kinship
458 coefficients greater than 0.0884 and were removed for downstream EEMS analysis and
459 haplotype construction and clustering.

460

461 **Estimating Effective Migration Surfaces**

462 We estimated migration and diversity relative to geographic distance using the estimating
463 effective migration surfaces (EEMS) method.[28] We applied EEMS to Genographic individuals
464 that were classified under African, European, and Native American ancestries. We excluded
465 East Asian and South Asian ancestries due to low sample size and population density. We first
466 computed pairwise genetic dissimilarities for all unrelated individuals with available postal code
467 data in each of the three ancestries using the *bed2diffs* tool provided with EEMS. We then ran
468 the EEMS algorithm with the *runeems_snps* tool and set the number of demes to 500. Per the
469 recommendation in the manual, we adjusted the variance for all proposed distributions of
470 diversity, migration, and degree-of-freedom parameters such that all were accepted 10%-40%
471 of the time. We increased the number of Markov chain Monte Carlo (MCMC) iterations until the
472 MCMC converged.

473

474 **Haplotype Calling and Network Construction**

475 We used IBDSeq version r1206 to generate shared identity-by-descent (IBD) segments from
476 genotype data for all unrelated individuals.[43] Unlike other algorithms for IBD detection, IBDseq
477 does not reply on phased genotype data and therefore is less susceptible to switch errors in
478 phasing that can cause erroneous haplotype breaks. We filter individual IBD segments by
479 length, excluding those shorter than 3cM. We also removed IBD segments that overlapped
480 partially or fully with long regions (1 Mb) of the chromosome that exhibited no SNPs across all
481 unrelated individuals in the Genographic dataset. These sites can result in false positives IBD
482 sharing and likely correspond to centromeres and telomeres.

483

484 We calculate the cumulative IBD sharing between individuals by summing the length of all
485 shared IBD segments. We limit our analysis to pairs of individuals in which cumulative IBD
486 sharing is ≥12 cM and ≤72 cM, as previously described.[9] We then constructed a haplotype
487 network of unrelated individuals by defining each node as an individual and the edge connecting
488 two vertices as the cumulative IBD sharing between two individuals, as a proportion of total

489 possible IBD sharing. For comparison, we also constructed an network without filtering for
490 minimum or maximum IBD sharing.
491
492 **Detection of IBD Clusters**
493 To identify clusters of related individuals in the haplotype network described above, we used the
494 Louvain Method for community detection implemented in the *igraph* package for R. Briefly, the
495 Louvain Method is a greedy iterative algorithm that assigns vertices of a graph into clusters to
496 optimize modularity (a measure of the density of edges within a community to edges between
497 communities). The Louvain Method begins by first assigning each node as its own community
498 and then adds node *i* to a neighbor community *j.* It then calculate the change in modularity and
499 places *i* in the community with that maximizes modularity. The algorithm terminates when no
500 vertices can be reassigned.
501
502 We partitioned the haplotype network into clusters by recursively applying the Louvain Method
503 within subcommunities. At the highest level, we take the full, unpartitioned haplotype graph and
504 identify a set of subcommunities. We isolate the vertices within each subcommunity, keeping
505 only the edges between those vertices to create separate new networks. We then apply the
506 Louvain Method to the new subgraphs. We repeat this process up to four levels. We combined
507 subcommunities with low genetic divergence based on F_{ST} values of < 0.0001 (see Genetic
508 Divergence) and arrive at a total of 25 clusters for the filtered network (≥12 cM and ≤72 cM). For
509 the unfiltered network, we arrived at 32 clusters, 4 of which contained less than 10 individuals
510 and were removed from subsequent analyses.
511
512 **Annotation of IBD Clusters**
513 We used a combination of ancestral birth origins and self-reported ethnicities to discern
514 demographic characteristics of each cluster. For each cluster, we quantified the proportion of
515 each birth origin (i.e. country of origin) amongst all four grandparents, treating each
516 grandparent's origin equality. We use these proportions to inform population labels. Clusters in
517 which a single non-US birth origin was in high proportions was labeled with that country. In
518 cases where multiple non-US birth locations exists in approximately equally high proportions,
519 we assigned a label representing the broader region (e.g. Eastern Europeans for Poland,
520 Lithuania, Ukraine, and Slovakia; East Asia for Japan, China). For certain clusters, annotations
521 could not be easily discerned by birth origin data. In these cases, we relied on self-reported
522 ethnicities to label the clusters as these populations were found to be less associated with a

523 non-US country (e.g. Ashkenazi Jews) or the population has resided in the US for generations
524 (African Americans, Acadians).
525
526 Annotations for the 25 clusters from the filtered network were found to be more interpretable
527 than annotations for the 28 clusters from the unfiltered networks. Specifically, many of the
528 clusters from the unfiltered networks exhibited similar proportions of ancestral origins or
529 ethnicities and were difficult to differentiate **(Table S2 and S3)**. Certain populations (e.g. Finns,
530 Middle Easterners) found from the filtered network were also not identified from the unfiltered
531 network. We therefore used the 25 clusters from the filtered network in downstream analyses.
532
533 **Mapping IBD Clusters**
534 We mapped individuals using their present-day geographic location. We aggregated individuals
535 from the same county using the postal code to county FIPS code mapping provided by the US
536 Census, and we identified the longitude and latitude points of each county using the same data
537 from the US Census. We then counted the number of individuals at each coordinate for each
538 ancestry.
539
540 To identify locations where a cluster is enriched, we performed a Fisher's exact test for each
541 location and ancestry to obtain an odds ratio and significance value. For each cluster, we
542 mapped only counties with statistically significant ($p<0.05$) enrichment and an odds ratio (OR) of
543 greater than 1. The size of the circles is scaled to the number of individuals in each location.
544
545 **Runs of Homozygosity**
546 We used PLINK v1.90b3.39 to infer runs of homozygosity with a window of 25 SNPs.[41] We
547 calculated the cumulative runs of homozygosity (cROH) size by summing the lengths of
548 homozygous segments.
549
550 **Haplotype Estimation**
551 Genographic genotypes were phased with the Sanger Imputation Service using EAGLE2 and
552 the Haplotype Reference Consortium reference panel.[44] No genotype imputation was
553 performed.
554
555 **Local Ancestry Inference**

556 We inferred local ancestry with RFMix v1.5.4 for Genographic samples in haplotype clusters
557 that were annotated as Hispanics/Latinos and African Americans.[32] We used samples of African
558 (AFR; N = 661), European (EUR; N = 503), and Native American (AMR; N = 347) ancestry from
559 the 1000 Genomes Project as the reference population. Specifically, we used LWK, MSL, GWD,
560 YRI, ESN, ACB, and ASW as reference African populations; CEU, GBR, FIN, IBS, and TSI as
561 reference European populations; and MXL, PUR, CLM, and PEL as reference Native American
562 populations.
563
564 RFMix was run using the default minimum window size of 0.2 cM and a node size of 5 to reduce
565 bias in the random forest model as a result of an unbalanced reference panel. We specifically
566 ran RFMix with the following flag: -w 0.2, -n 5. Global ancestry proportions were derived by
567 quantifying the proportions of total local ancestry tracts for each ancestry.
568
569 **Genetic Divergence**
570 We computed weighted Weir-Cockerham F_{ST} estimates for each pair of haplotype clusters using
571 PLINK v1.90b3.39.[41] Using the distance matrix of F_{ST} values between clusters, we constructed
572 an unrooted phylogenetic tree using the neighbor joining method implemented in *scikit-bio*.[45] We
573 visualized the tree using Interactive Tree Of Life.[46]
574
575
576

Data and Code Availability

Genotype data and associated metadata are available to researchers through an application process and data usage agreement. We encourage qualified researchers to email the Genographic team at National Geographic Society (genographic@ngs.org) for information on and access to the Genographic database.

Custom scripts generated to analyze the data in this paper are available through GitHub (https://github.com/chengdai/genographic_ancestry).

Acknowledgement

We thank the National Geographic Genographic Project participants who consented to research participations for making this study possible. We also thank Gregory Vilshansky for helping organize and manage the data for the Genographic Project.

This work was supported by funding from the National Institutes of Health (K99MH117229 to A.R.M.). C.L.D., M.M., R.T., and C.R. would also like to thank all the members of the MIT Senseable City Lab Consortium for supporting this research, including Allianz, Amsterdam Institute for Advanced Metropolitan Solutions, Brose, Cisco, Ericsson, Fraunhofer Institute, Liberty Mutual Institute, Kuwait-MIT Center for Natural Resources and the Environment, Shenzhen, Singapore-MIT Alliance for Research and Technology (SMART), Uber, Victoria State Government, Volkswagen Group America. M.G.V. acknowledges support from the National Geographic Society.

Author Contributions

C.L.D. and A.R.M. designed the study, performed research, and wrote the manuscript. M.G.V. coordinated and supervised the data gathering for the Genographic Project. M.M.V., C.H.Y., and R.T. contributed to the data aggregation and data analysis. A.R.M., C.R. and M.J.D. supervised research. All authors reviewed the manuscript.

Conflicts of Interest

M.G.V. is the Senior Program Officer for the National Geographic Society and lead scientist for the Genographic Project.

References

611 1. The 1000 Genomes Project Consortium. A global reference for human genetic variation.
612 *Nature* **526**, 68–74 (2015).
613 2. Tishkoff, S. A. *et al.* The Genetic Structure and History of Africans and African Americans.
614 *Science* **324**, 1035–1044 (2009).
615 3. Bryc, K. *et al.* Genome-wide patterns of population structure and admixture in West Africans
616 and African Americans. *Proc. Natl. Acad. Sci.* **107**, 786–791 (2010).
617 4. Bryc, K. *et al.* Genome-wide patterns of population structure and admixture among
618 Hispanic/Latino populations. *Proc. Natl. Acad. Sci.* **107**, 8954–8961 (2010).
619 5. Reich, D. *et al.* Reconstructing Native American population history. *Nature* **488**, 370–374
620 (2012).
621 6. Novembre, J. *et al.* Genes mirror geography within Europe. *Nature* **456**, 98–101 (2008).
622 7. Hellenthal, G. *et al.* A Genetic Atlas of Human Admixture History. *Science* **343**, 747–751
623 (2014).
624 8. Baharian, S. *et al.* The Great Migration and African-American Genomic Diversity. *PLOS*
625 *Genet.* **12**, e1006059 (2016).
626 9. Han, E. *et al.* Clustering of 770,000 genomes reveals post-colonial population structure of
627 North America. *Nat. Commun.* **8**, 14238 (2017).
628 10. Bryc, K., Durand, E. Y., Macpherson, J. M., Reich, D. & Mountain, J. L. The Genetic
629 Ancestry of African Americans, Latinos, and European Americans across the United States.
630 *Am. J. Hum. Genet.* **96**, 37–53 (2015).
631 11. Ramachandran, S. *et al.* Support from the relationship of genetic and geographic distance in
632 human populations for a serial founder effect originating in Africa. *Proc. Natl. Acad. Sci.* **102**,
633 15942–15947 (2005).
634 12. Wang, S. R. *et al.* Simulation of Finnish Population History, Guided by Empirical Genetic
635 Data, to Assess Power of Rare-Variant Tests in Finland. *Am. J. Hum. Genet.* **94**, 710–720
636 (2014).
637 13. Bray, S. M. *et al.* Signatures of founder effects, admixture, and selection in the Ashkenazi
638 Jewish population. *Proc. Natl. Acad. Sci.* **107**, 16222–16227 (2010).
639 14. Mooney, J. A. *et al.* Understanding the Hidden Complexity of Latin American Population
640 Isolates. *Am. J. Hum. Genet.* **103**, 707–726 (2018).
641 15. Belbin, G. M. *et al.* Genetic identification of a common collagen disease in Puerto Ricans via
642 identity-by-descent mapping in a health system. *eLife* **6**, e25060 (2017).
643 16. Popejoy, A. B. & Fullerton, S. M. Genomics is failing on diversity. *Nat. News* **538**, 161
644 (2016).

645 17. Martin, A. R. *et al.* Current clinical use of polygenic scores will risk exacerbating health
646 disparities. *bioRxiv* 441261 (2019). doi:10.1101/441261
647 18. Caswell-Jin, J. L. *et al.* Racial/ethnic differences in multiple-gene sequencing results for
648 hereditary cancer risk. *Genet. Med. Off. J. Am. Coll. Med. Genet.* **20**, 234–239 (2018).
649 19. Martin, A. R. *et al.* Human Demographic History Impacts Genetic Risk Prediction across
650 Diverse Populations. *Am. J. Hum. Genet.* **100**, 635–649 (2017).
651 20. Manrai, A. K. *et al.* Genetic Misdiagnoses and the Potential for Health Disparities. *N. Engl.*
652 *J. Med.* **375**, 655–665 (2016).
653 21. Morales, J. *et al.* A standardized framework for representation of ancestry data in genomics
654 studies, with application to the NHGRI-EBI GWAS Catalog. *Genome Biol.* **19**, (2018).
655 22. Behar, D. M. *et al.* The Genographic Project Public Participation Mitochondrial DNA
656 Database. *PLOS Genet.* **3**, e104 (2007).
657 23. Elhaik, E. *et al.* The GenoChip: A New Tool for Genetic Anthropology. *Genome Biol. Evol.* **5**,
658 1021–1031 (2013).
659 24. Alexander, D. H., Novembre, J. & Lange, K. Fast model-based estimation of ancestry in
660 unrelated individuals. *Genome Res.* **19**, 1655–1664 (2009).
661 25. Abraham, G., Qiu, Y. & Inouye, M. FlashPCA2: principal component analysis of Biobank-
662 scale genotype datasets. *Bioinformatics* **33**, 2776–2778 (2017).
663 26. McInnes, L. & Healy, J. UMAP: Uniform Manifold Approximation and Projection for
664 Dimension Reduction. *ArXiv180203426 Cs Stat* (2018).
665 27. Diaz-Papkovich, A., Anderson-Trocme, L. & Gravel, S. Revealing multi-scale population
666 structure in large cohorts. (2018). doi:10.1101/423632
667 28. Petkova, D., Novembre, J. & Stephens, M. Visualizing spatial population structure with
668 estimated effective migration surfaces. *Nat. Genet.* **48**, 94–100 (2016).
669 29. US Census Bureau. The Great Migration, 1910 to 1970. *U.S. Census* Available at:
670 https://www.census.gov/dataviz/visualizations/020/. (Accessed: 21st February 2019)
671 30. Massey, D. S., Rugh, J. S. & Pren, K. A. The Geography of Undocumented Mexican
672 Migration. *Mex. Stud. Mex.* **26**, 129–152 (2010).
673 31. Blondel, V. D., Guillaume, J.-L., Lambiotte, R. & Lefebvre, E. Fast unfolding of communities
674 in large networks. *J. Stat. Mech. Theory Exp.* **2008**, P10008 (2008).
675 32. Maples, B. K., Gravel, S., Kenny, E. E. & Bustamante, C. D. RFMix: A Discriminative
676 Modeling Approach for Rapid and Robust Local-Ancestry Inference. *Am. J. Hum. Genet.* **93**,
677 278–288 (2013).
678 33. Passel, J. S. & Fix, M. U.S. Immigration in a Global Context: Past, Present, and Future.

Indiana J. Glob. Leg. Stud. **2**, 5–19 (1994).

34. Grieco, E. M., Trevelyan, E., Larsen, L., Acosta, Y. D. & Gambino, C. The Size, Place of Birth, and Geographic Distribution of the Foreign-Born Population in the United States: 1960 to 2010. *Popul. Div. Work. Pap. No 96 US Census Bur.* 38
35. Pemberton, T. J. *et al.* Genomic Patterns of Homozygosity in Worldwide Human Populations. *Am. J. Hum. Genet.* **91**, 275–292 (2012).
36. Moorjani, P. *et al.* Genetic Evidence for Recent Population Mixture in India. *Am. J. Hum. Genet.* **93**, 422–438 (2013).
37. Tadmouri, G. O. *et al.* Consanguinity and reproductive health among Arabs. *Reprod. Health* **6**, 17 (2009).
38. Hussain, R. & Bittles, A. H. Assessment of association between consanguinity and fertility in Asian populations. *J. Health Popul. Nutr.* **22**, 1–12 (2004).
39. Erlich, Y., Shor, T., Pe'er, I. & Carmi, S. Identity inference of genomic data using long-range familial searches. *Science* **362**, 690–694 (2018).
40. Regalado, A. More than 26 million people have taken an at-home ancestry test. *MIT Technology Review* Available at: https://www.technologyreview.com/s/612880/more-than-26-million-people-have-taken-an-at-home-ancestry-test/. (Accessed: 21st February 2019)
41. Purcell, S. *et al.* PLINK: a tool set for whole-genome association and population-based linkage analyses. *Am. J. Hum. Genet.* **81**, 559–575 (2007).
42. Manichaikul, A. *et al.* Robust relationship inference in genome-wide association studies. *Bioinformatics* **26**, 2867–2873 (2010).
43. Detecting identity by descent and estimating genotype error rates in sequence data. - PubMed - NCBI. Available at: https://www.ncbi.nlm.nih.gov/pubmed/24207118. (Accessed: 21st February 2019)
44. McCarthy, S. *et al.* A reference panel of 64,976 haplotypes for genotype imputation. *Nat. Genet.* **48**, 1279–1283 (2016).
45. Saitou, N. & Nei, M. The neighbor-joining method: a new method for reconstructing phylogenetic trees. *Mol. Biol. Evol.* **4**, 406–425 (1987).
46. Letunic, I. & Bork, P. Interactive tree of life (iTOL) v3: an online tool for the display and annotation of phylogenetic and other trees. *Nucleic Acids Res.* **44**, W242-245 (2016).

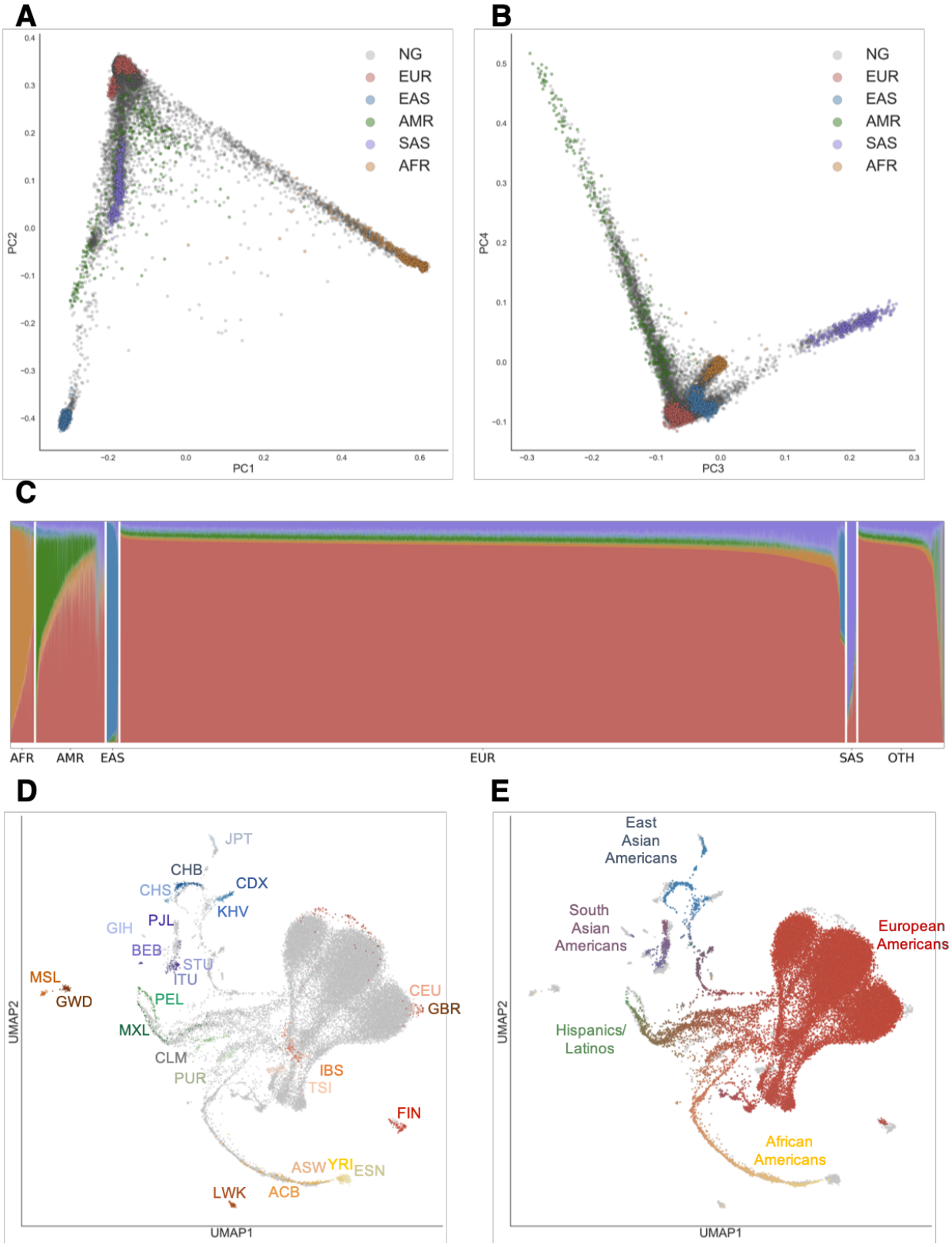
A
NG
EUR
EAS
AMR
SAS
AFR
PC1
PC2
B
PC3
PC4
C
AFR
AMR
EAS
EUR
SAS
OTH
D
JPT
CHB
CHS
CDX
KHV
GIH
PJL
BEB
STU
ITU
MSL
GWD
PEL
MXL
CLM
PUR
CEU
GBR
IBS
TSI
FIN
ASW
YRI
ESN
LWK
ACB
UMAP1
UMAP2
E
East Asian Americans
South Asian Americans
European Americans
Hispanics/ Latinos
African Americans
UMAP1
UMAP2

712

713 **Figure 1. Genetic Diversity of the US Population**

714 (A) Principal Components Analysis (PCA) of individuals in the United States and in the 1000
715 Genome Project. Each individual is represented by a single dot. Individuals in this study are
716 colored in grey while 1000 Genome Population individuals are colored by super population
717 (EUR = European, AFR = African, AMR = Admixed American, EAS = East Asian, SAS = South
718 Asian). Principal components (PC) 1 and PC2 are shown.

719 (B) Similar to (A), with PC3 and PC4 shown.

720 (C) ADMIXTURE analysis at K=5 of individuals in this study. Each individual was assigned a
721 continent-level ancestry label using a Random Forest model trained on the super population
722 labels and the first 10 PCs of the 1000 Genome Project dataset. OTH = individuals who did not
723 meet the 90% confidence threshold for classification.

724 (D) UMAP projection of the first 20 PCs. Each dot represents one individual. In (D), individuals
725 in the 1000 Genomes Project are colored by population, while Genographic Project individuals
726 from this study are in grey. In (E), 1000 Genome Project individuals are colored in grey while
727 Genographic Project individuals are colored based on their admixture proportions from
728 ADMIXTURE. The color for each dot was calculated as a linear combination of each individual's
729 admixture proportion and the RGB values for the colors assigned to each continental ancestry
730 (EUR = red, AFR = yellow, NAT or Native American = green, EAS = blue, SAS = purple).
731 Distances in UMAP do not directly correspond to genetic distance. See Materials and Methods
732 for specific population labels.

733

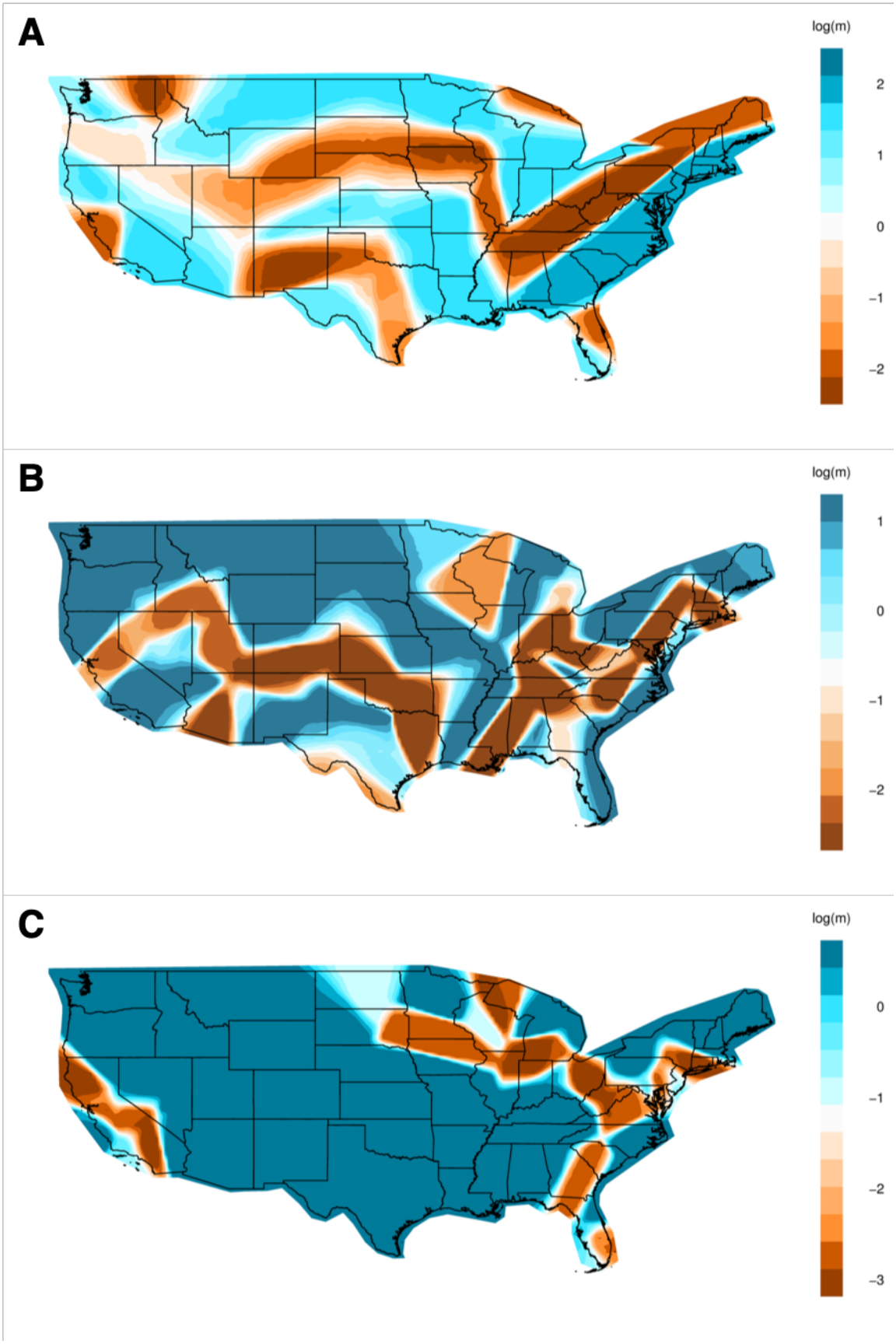

734

735 **Figure 2. Migration Rates of African Americans, Hispanics/Latinos, and Europeans within**
736 **the United States.**
737 (A) - (C) Migration rates inferred with EEMS for African Americans (A), Hispanics/Latinos (B),
738 and Europeans (C). Colors and values correspond to inferred rates, *m*, relative to the overall
739 migration rate across the country. Shades of blue indicate logarithmically higher migration (i.e.
740 log(m) = 1 represents effective migration that is ten-fold faster than the average) while shades
741 of orange indicate migration barriers.
742

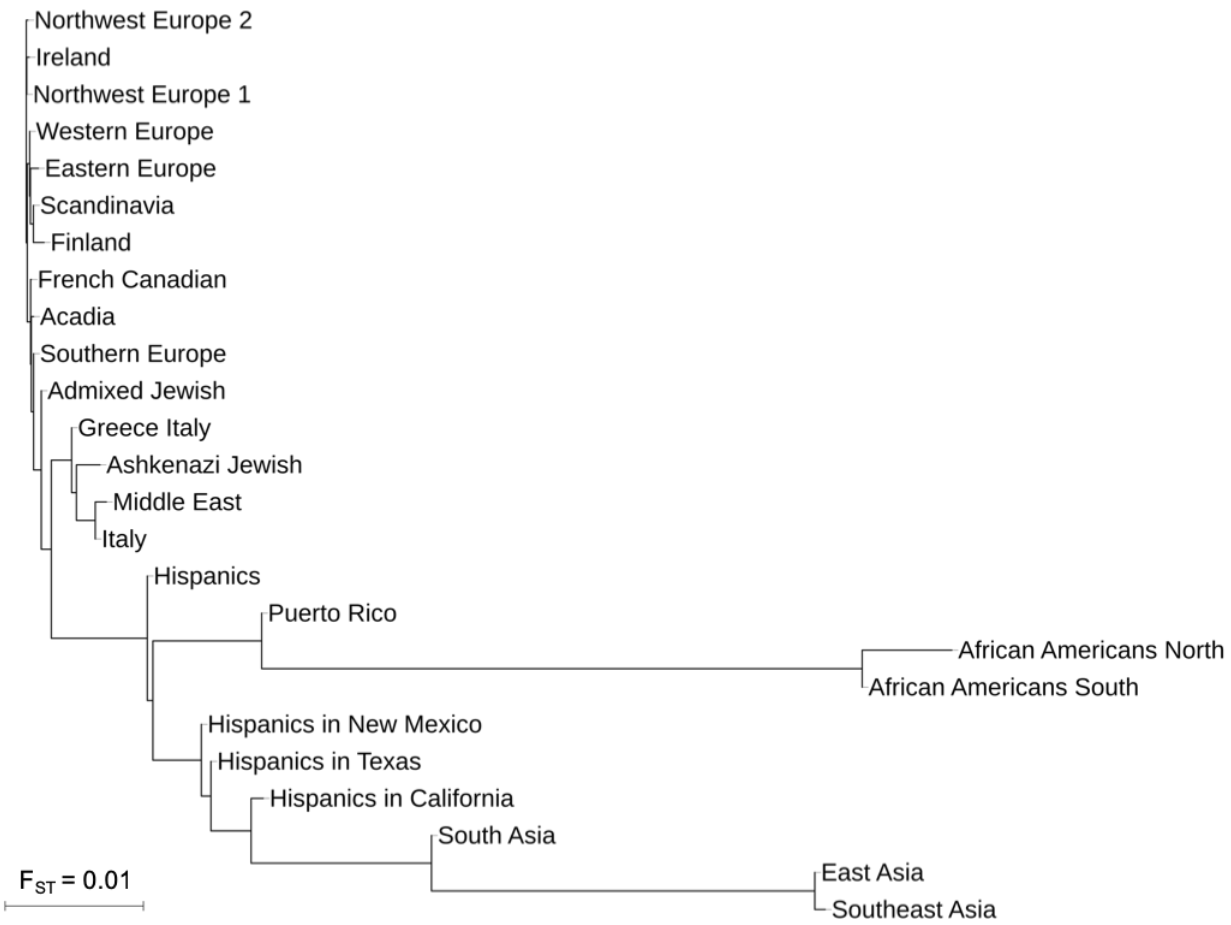

Figure 3. Genetic differentiation of haplotype clusters

Unrooted phylogenetic tree of haplotype clusters was constructed using the neighbor joining method with F_{ST} as genetic distance. Negative branch lengths were converted to zero.

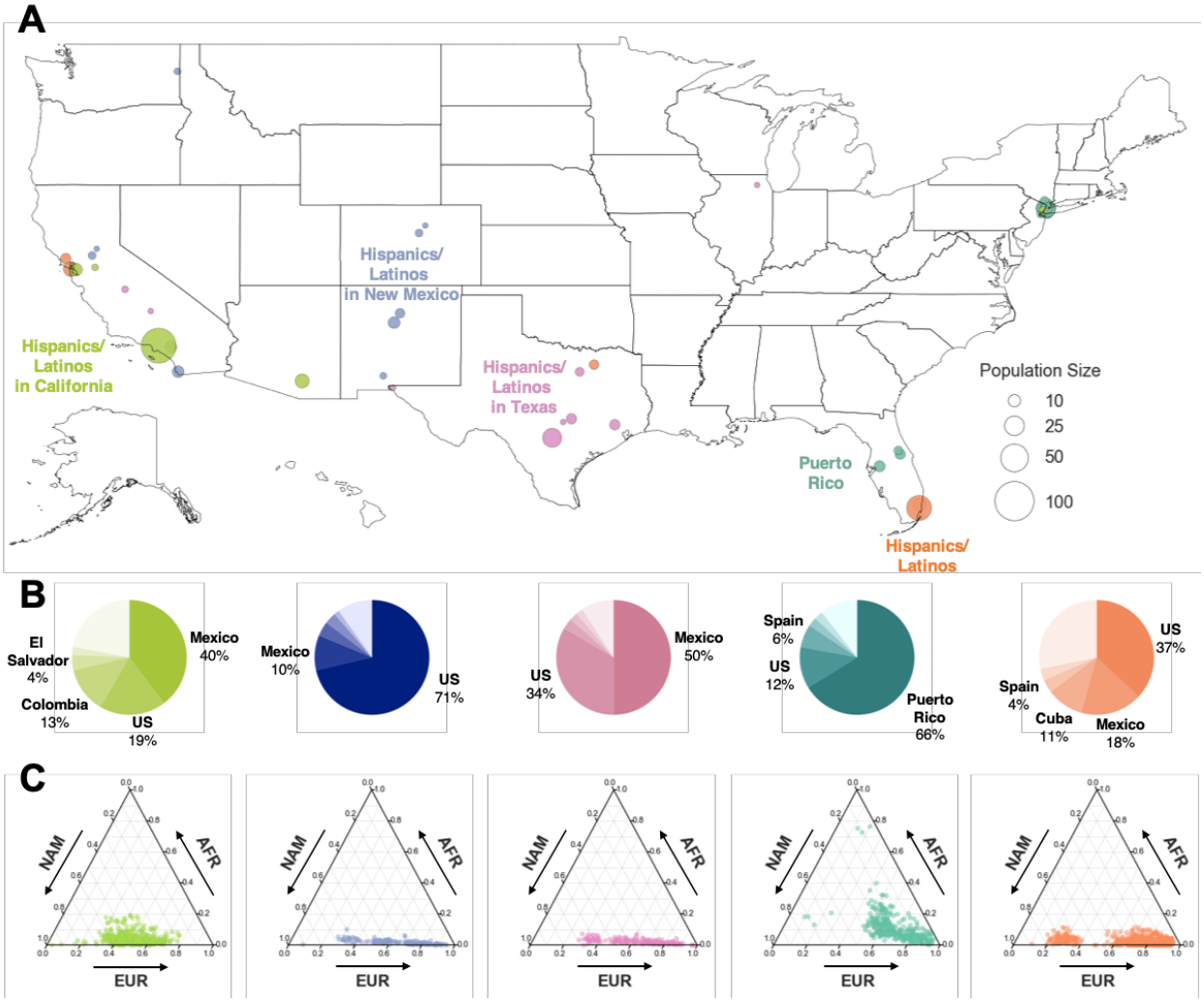

Figure 4. Distribution of Hispanic/Latino Haplotype Clusters

(A) Map of counties in which Hispanic/Latino haplotype clusters are enriched. Each dot corresponds to a county, and the size of the dot signifies the number of samples of the particular cluster in that county. Only the Hispanic/Latino cluster with the highest odds ratio is shown for each county, and only the top ten locations with the highest odds ratios are shown for each cluster. Maps showing the full distribution for each haplotype cluster can be found in the supplement (**Figure S6**).

(B) Ancestral birth origin proportions of each cluster for individuals with complete pedigree annotations, up to grandparent level. Proportions were calculated from aggregating the birth locations of all grandparents corresponding to members of each haplotype cluster. For each chart, only the top five birth origins are shown as individual slices; the remaining birth origins are aggregated into one slice (lightest color).

(C) Ternary plots of ancestry proportions based on local ancestry inference for each haplotype cluster. Each dot represents one individual.

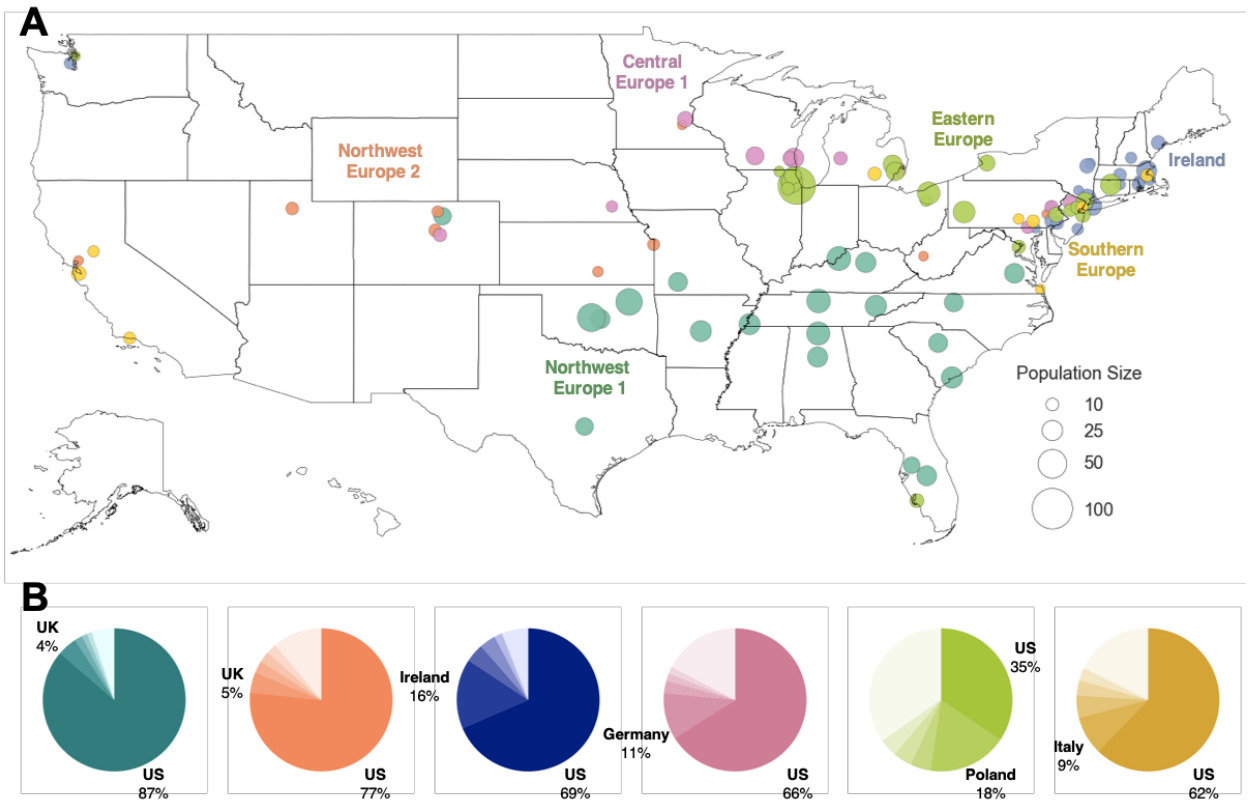

Figure 5. Distribution of European American Haplotype Clusters

(A) Geographic distributions of haplotype clusters corresponding to regional European ancestries. Each county containing present-day individuals is represented by a dot. The top 20 locations with the highest odds ratio are shown for each cluster. Maps showing the full distribution for each cluster can be found in the supplement (**Figure S6**).

(B) Ancestral birth origin proportions for each cluster in (A). Only individuals with complete pedigree annotations, up to grandparent level, are included. For each chart, only the top five birth origins are visualized as individual slices; the remaining birth origins are aggregated into one slice (lightest color).

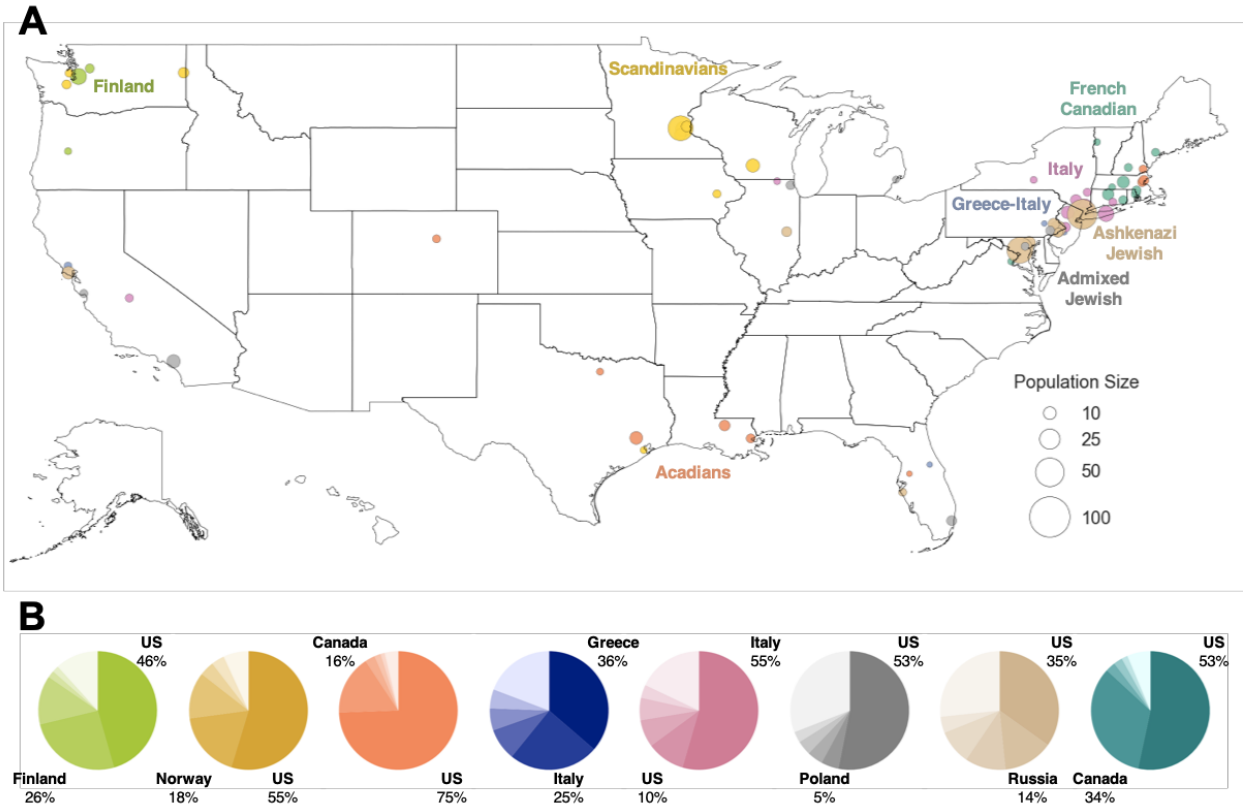

Figure 6. Distribution of European American Haplotype Clusters

(A) Present-day location of individuals in clusters of more genetically isolated European populations, similar to Figure 5A. For clarity, the top ten locations with the highest odds ratio are shown for each cluster.

(B) Ancestral birth origin proportions for each cluster in (A). Only individuals with complete pedigree annotations, up to grandparent level, are shown. For each chart, only the top five birth origins are shown as individual slices; the remaining birth origins are aggregated into one slice (lightest color).

Cluster	Samples	Median Cumulative ROH	Median Cumulative IBD
Northwest Europe 1	11,725	2.88	15.23
Northwest Europe 2	1,571	2.80	15.15
Ireland	2,137	2.85	15.42
Central Europe	3,116	2.83	15.06
Eastern Europe	2,471	3.16	15.37
Southern Europe	1,626	2.73	14.98
Italy	697	6.91	14.64
Greece-Italy	238	7.28	15.02
Scandinavia	717	3.02	15.54
Finland	314	3.67	17.50
Acadia	249	3.89	19.48
French Canadian	314	2.89	16.60
Ashkenazi Jewish	1,475	11.26	31.75
Admixed Jewish	445	2.75	15.50
Hispanics/Latinos	810	3.53	16.38
Hispanics/Latinos in California	573	4.10	17.11
Hispanics/Latinos in New Mexico	163	5.52	21.92
Hispanics/Latinos in Texas	177	6.27	23.65
Puerto Rico	350	8.01	26.23
African Americans South	761	3.34	19.56
African Americans North	420	2.94	15.90
East Asia	561	3.65	19.63
Southeast Asia	325	8.44	17.90
South Asia	389	10.42	14.82
Greater Middle East	93	9.01	17.16

Table 1. Summary of Haplotype Clusters

Cumulative runs of homozygosity (cROH) was calculated by summing the regions of continuous homozygous segments. Cumulative IBD was determined by summing IBD segments of ≥ 3 cM and filtering for only pairs ≥ 12cM and ≤ 72 cM. Statistics were determined within haplotype clusters, rather than across the ancestrally heterogeneous and imbalanced full network.